DEVELOPMENT OF AN ADAPTIVE PID CONTROL SYSTEM FOR A THERMAL CHAMBER REFRIGERATED WITH A THERMOELECTRIC DEVICE

Douglas Iceri Lasmar, douglaslasmar@ufmg.br
Glayson dos Santos Cornélio, glaysoncornelio@yahoo.com.br
Cláudio Mendonça, com@ufmg.br
Mateus Reis, mateus.freis@gmail.com
Ricardo Nicolau Nassar Koury, koury@demec.ufmg.br
Antônio Augusto Torres Maia, aamaia@ufmg.br
Universidade Federal de Minas Gerais, Departamento de Engenharia Mecânica
Av.Antônio Carlos, 6627, Pampulha, 31270-901, Belo Horizonte – Minas Gerais - Brasil

Abstract: *Thermoelectric devices have been used to replace the conventional vapor compression refrigeration systems in small chambers and cooling surfaces. These devices have some better features such as no moving parts, quick response, silent operation and direct conversion of electric energy into heat. This last feature makes it easier to control the cooling capacity of systems based on thermoelectric devices. In this work, a PID controller, with adaptive gains, have been developed to regulate the cooling power in a small thermoelectric cooling chamber. From the thermal load estimation of the refrigerator, the controller gains are calculated at each operating condition. A power electronic circuit, controlled by a microcontroller, has been developed to control the thermoelectric module power. To validate the proposed controller, the control algorithm has been programmed in the microcontroller and tested under different operation conditions. The results obtained indicated that the proposed system is capable of controlling the capacity of the thermoelectric cooler with an acceptable performance. Using the step response curves, it was possible to determine the time constant, the settling time and the maximum overshoot to the adaptive and the non adaptive control system. Based on these final results it was concluded that the proposed method worked and the performance of adaptive control was better than the non adaptive.*

Keywords: *Peltier Effect; Temperature Control; Adaptive Control; PID Controller; Thermoelectricity.*

1. INTRODUCTION

Temperature is an important aspect in several research and manufacturing processes and, several times, its correct control and adjustment may determine the final product quality. The thermally sensitive processes can be harmed by manual control procedures due to the needs of temperature changing, precise control and even system stabilization.

There are many different types of refrigerating systems available nowadays. Among of then it is worth to mention the refrigerating systems based on thermoelectric devices. These systems have some important characteristics that should be highlighted like the direct conversion of electric energy into heat, it has no moving parts and its operation is silent. In addition, traditional components present in the vapor compression systems, for example, such as the compressor, the condenser, the evaporator and the expansion valve, can be reduced to a single peltier effect chip.

In this work it was built a thermal chamber that uses a thermoelectric device to control internal temperature. The internal and external temperatures were monitored by sensors and an electronic control circuit was developed to adjust the power of the actuator regarding to the temperature inside the chamber.

The developed controller was a PID with adaptive gains. To calculate the controller gains were used the automatic adjustment rules provided by Vilanova (2008), for first order systems with time delay. The controller gains were calculated for each operating point, depending on the thermal load that the system was subjected.

The plant characteristics at different operating points have been validated employing step response tests, as described by Lio et al. (2009), and the controller implementation has been based on the output equations of the Proportional-Integral-Derivative controller described by Maia (2010). Additionally, improvement techniques, such as anti-windup described by Visioli (2003), complemented the work.

2. EXPERIMENTAL APPARATUS

The thermal chamber, shown in Fig. 1, consists of a box where the walls are composed of three different materials: aluminum, glass wool and polycarbonate. The front side of the chamber was built using two sheets of translucent acrylic, with the space between them filled with air, and allowing internal monitoring of the chamber. On the back side of the chamber there is an opening where the thermoelectric module and the air-cooled heat exchangers are assembled, both internally (Fig. 2) and externally. The chamber also has four temperature transducers, the first one is internal and positioned in the center of the chamber, the second is fixed internally to the right wall, the third one is fixed externally

at the top wall (Fig. 1) and the fourth transducer is positioned externally away from the chamber to measure the ambient temperature. On the back of the refrigerator was positioned the control circuit, as well as the drive circuit of the thermoelectric modules.

Figure 1. Thermal Chamber

A set of six 100ohm and 25W resistors connected in parallel and an adjustable voltage source were used to simulate different thermal loads. Due the low impedance of wiring used compared to resistive load, it was considered that the power supplied by the source was fully converted in heat, by joule effect, in the resistive loads.

Figure 2. Resistive assembly for the thermal load variation

To monitor the temperatures, four electronic LM135 transducers were used. The LM135 operate as a 2-terminal zener diode, were the breakdown voltage is directly proportional to absolute temperature (National, 2008). To read the data from the sensors, convert them into temperature, calculate the control signal and do corrections in the actuator power, a microcontroller PIC18f452 was used. In Fig. 3 it is presented a connection schematic from the LM135 sensors to the microcontroller.

For local access to system information, a display of two rows and sixteen columns was used. Moreover, the system has an asynchronous full duplex serial output that allows sending detailed information to a microcomputer, which makes the construction of response curves to variations in thermal load easier. To match the logic levels of the microcontroller and the computer and to establish communication between them, a MAX232 integrated circuit was used.

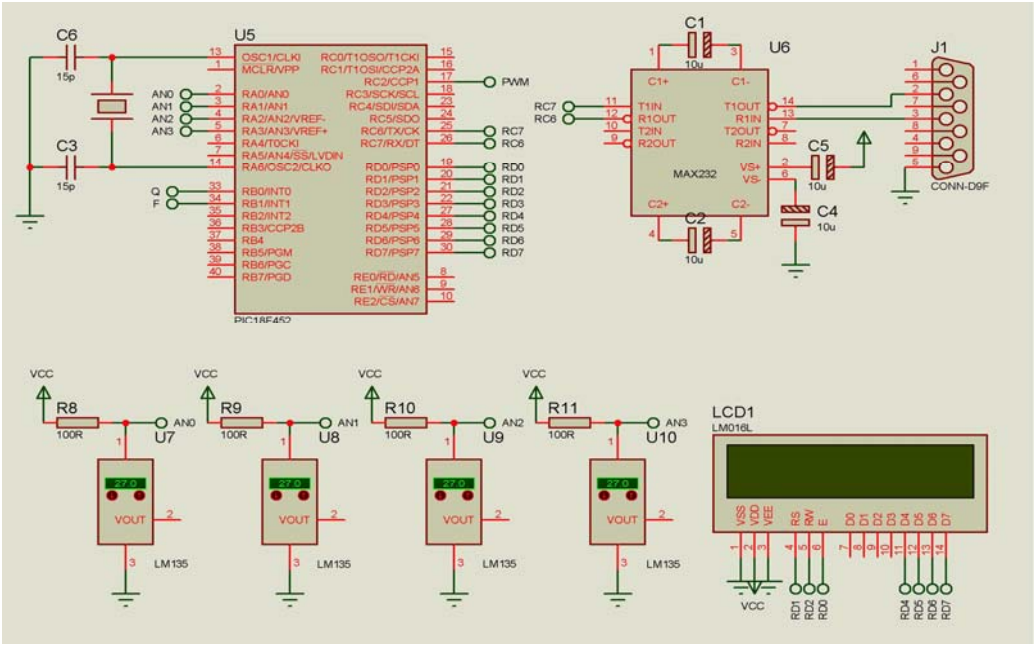

Figure 3. Electronic circuit of control, monitoring and communication

The direction of heat flow, supplied or withdrawn by the thermoelectric module and determined by the microcontroller, is performed by four mosfets arranged in an H bridge configuration, as shown in Fig.4. When the optocouplers U1 and U4 are simultaneously activated, the mosfets Q1 and Q4 are excited, allowing the passage of electric current in the direction defined as positive, causing heat to be supplied to the chamber. Similarly, when the optocouplers U3 and U2 are triggered, the mosfets Q2 and Q3 are excited, forcing the flow of electric current in the direction defined as negative, removing, thus, heat from inside the chamber.

The electric current intensity supplied to the module, and therefore the amount of heat removed from or supplied to the chamber, is controlled by the excitation of the transistor Q6, which controls the mosfet Q5. The microcontroller was adjusted to maintain the PWM output with a fixed oscillation at 244Hz, and during an oscillation period (duty cycle), the time that the output remains at high and low logic levels determines the current intensity.

The optocouplers U1, U2, U3 and U4, as well as the transistor Q6 were used to amplify the logic signals provided by the microcontroller to the level necessary for the correct saturation of the mosfets Q1, Q2, Q3, Q4 and Q5.

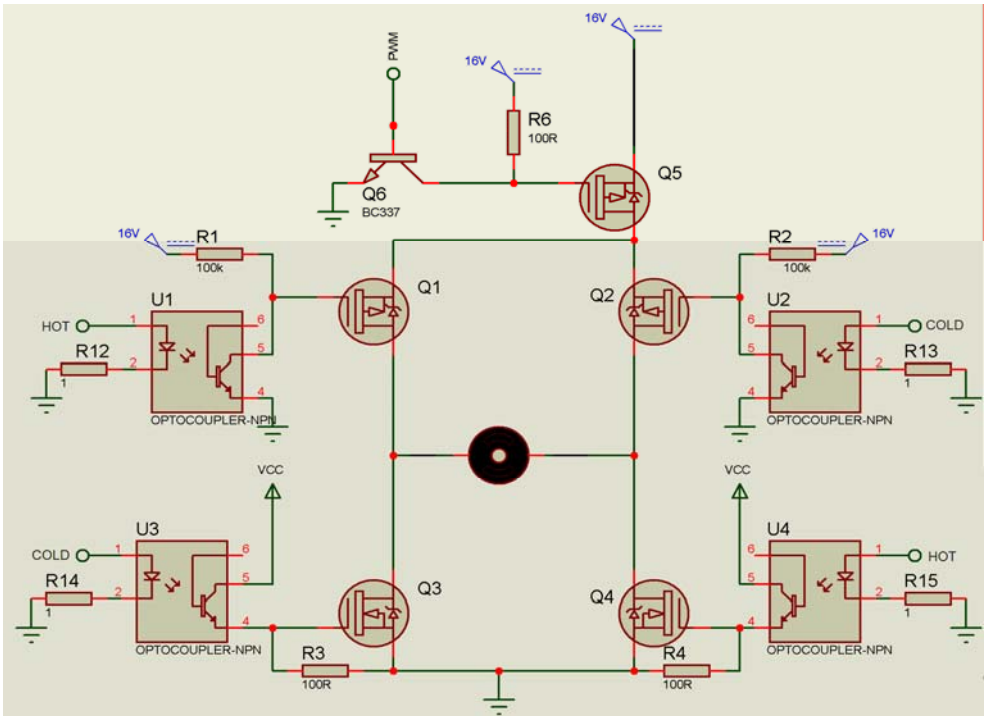

Figure 4 Electronic circuit of pumping heat

3. MODEL IDENTIFICATION

Initially, four tests were conducted to identify the system behavior and some physical characteristics of the chamber, pointing among them the thermal resistance of the walls and the settling time. After some preliminary studies with respect to the changes in thermal load, caused by the activation of the resistive assembly, step response tests were done at different operating points. These tests consisted of applying a known heat flow in the chamber (the voltage applied to the resistive load was adjusted to provide approximately 0W, 15W, 30W and 45W) while activating the thermoelectric module in 88% of its work cycle (equivalent to 900/1023 of the PWM resolution). After the temperature inside the chamber reaches equilibrium, the power applied to the module decreases to 63.5% (equivalent to 650/1023 of the PWM resolution) and the chamber behavior is monitored until it reaches equilibrium again. The Fig. 5 presents the results for the testes performed employing thermal load of 0W, 15W, 30W and 45W. It is observed in these tests, especially in tests with the thermal load of 0 and 45W, that the external temperature affects the internal temperature. However, high frequency oscillations from the air conditioning system, as those visualized in the curves of external temperature of the trials of 15 and 30W, do not affect substantially the characteristics of the internal temperature.

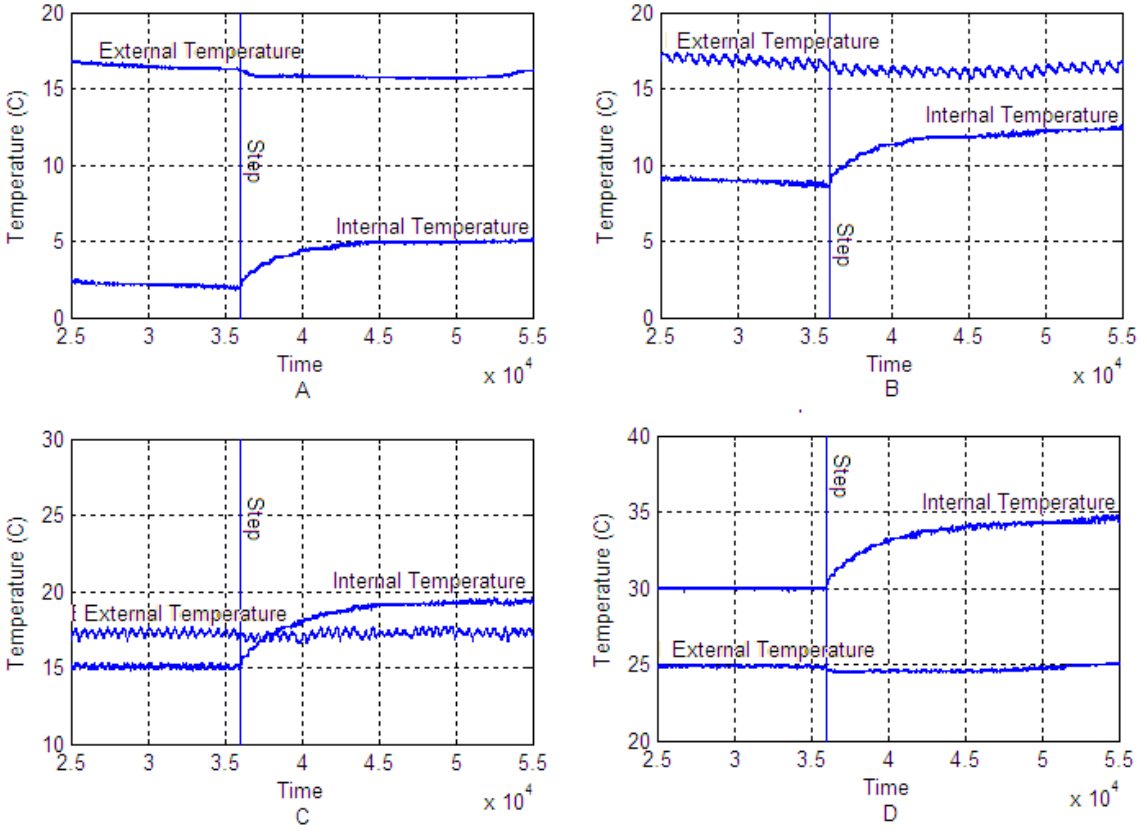

Figure 5 PWM Step Response for different Heat Loads, 0W (A), 15W (B), 30W (C) e 45W (D).

Augmenting the area close to the step it is possible to observe the delay in the system response. Fig. 6 shows the delay for the trials with a thermal load of 15W and 45W. These delays were, respectively, 22 and 37 seconds

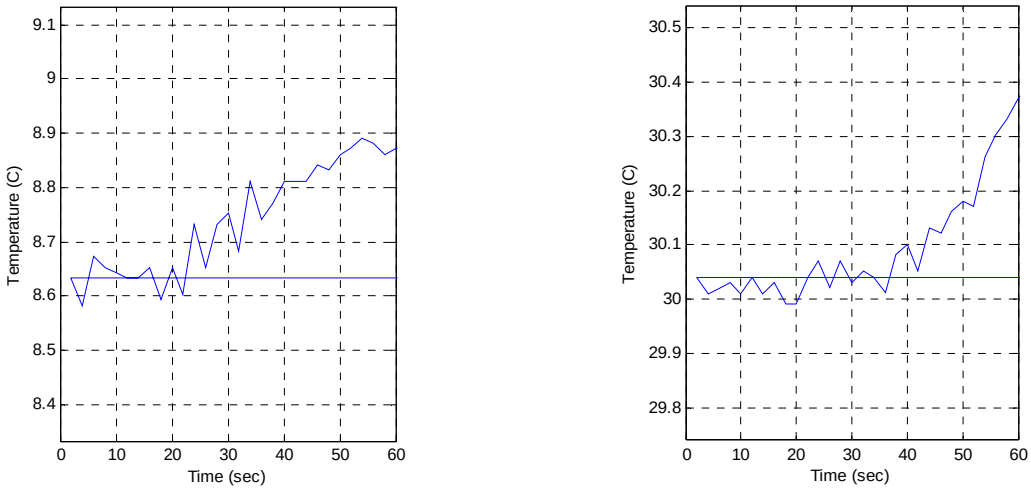

A B

Figure 6 Step Response Time Delay, (A) 15W e (B) 45W

From the step response curves for different thermal loads, it was possible to model the response of the internal temperature of the chamber wall as a first order transfer function plus delay time, equivalent to Eq. 1, where K represents the static gain, τ time constant, θ the time delay and "s" the Laplace operator.

$$G(s) = \frac{Ke^{-\theta s}}{(\tau s + 1)} \tag{1}$$

The results using thermal loads of 15 and 45W and their mathematical models, are presented in Fig. 7, where it is possible to note that, although the plant is the same, it presents different characteristics (gain, time constant, time delay) for different operating points.

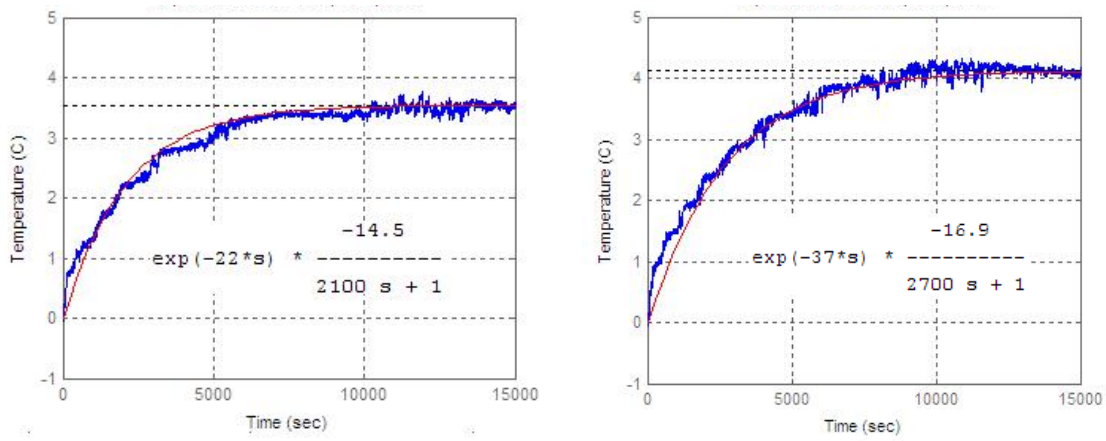

A B

Figure 7 First Order Mathematical Model for Some Points of Operation, (A) 15W and (B) 45W.

Using the information obtained from mathematical models and experimental data, it was possible to estimate mathematically the relation between the model variables (static gain, time constant and time delay) and the thermal load variation. Fig. 8 shows the value of these variables, as well as the interpolation curve. In this figure it is observed that, for the studied range of the thermal load (0 to 45W), both the time constant and the static gain increase in absolute value when the thermal load increases.

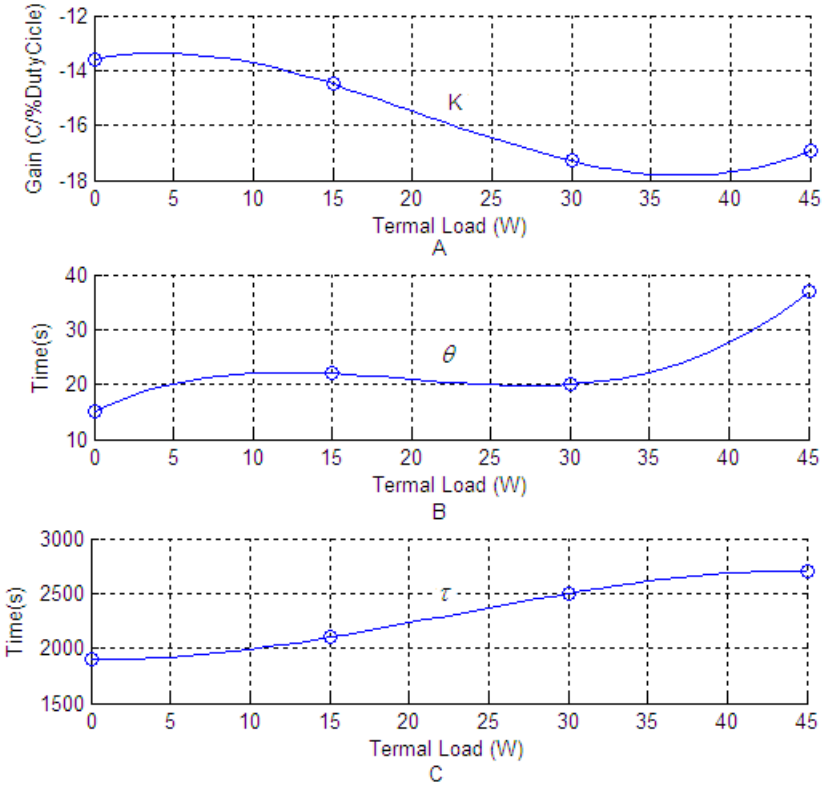

Figure 8. Variables Settings Curves, Static Gain (A), delay (B), Time Constant (C)

The Eq 2, 3 and 4 were determined from the curves shown in Fig.8 by a polynomial approximation. The values of K, τ and θ have been determined from the system thermal load throughout the operating range.

$$K = 0.0002\,X^3 - 0.0155\,X^2 + 0.1166\,X - 13.6000 \tag{2}$$

$$\tau = -0.0197X^3 + 1.3333X^2 - 2.2222X + 1899.9999 \tag{3}$$

$$\theta = 0.0013X^3 - 0.0822X^2 + 1.3888X - 14.9999 \tag{4}$$

4. CONTROLLER PARAMETERS

This work it was employed a PID controller parameterized employing the robust automatic adjustment rules described by Vila Nova (2008). The advantage of this strategy is that it enables the calculation of the controller optimum parameters for each operating point within the system operating range. Method is applicable to first order systems with time delay. The Eq. 5, 6, 7 and 8 are the equations of adjustments proposed by Villa Nova (2008) where K_p represents the proportional gain, T_i the integral time and T_d the derivative time. It can be observed that the variables used to adjust the controller parameters, K (static gain), τ (time constant) and θ (time delay), are obtained from Eq. 2, 3 and 4.

$$T_i = \tau + 0.03\,\theta \tag{5}$$

$$K_p = \frac{T_i}{2.65\;K\,\theta} \tag{6}$$

$$11 = \frac{\tau}{T_i} \tag{7}$$

$$\frac{T_d}{N} = 1.72\ \theta \tag{8}$$

The Fig. 9 shows the proposed controller block diagram. The block "Gain Scheduling" has the function to recalculate the controller gains from the transfer function.

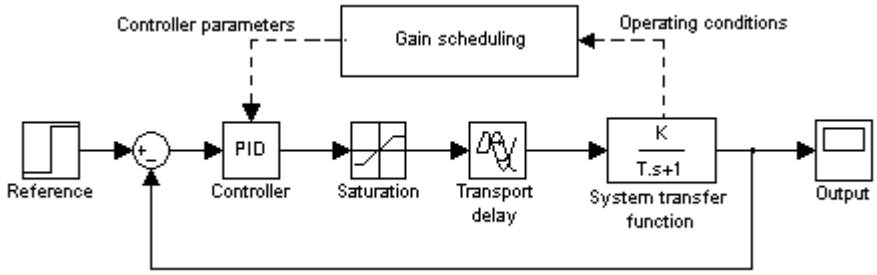

Figure 9 Plant Control and Parameterization Diagram

5. CONTROLLER ALGORITHM

There are several ways to express the PID controller (National, 2001; Ogata, 2003; Vilanova, 2008). In this work, the ideal typical controller was considered, as Eq. 9 and Eq. 10, where e(t) represents the error, SP the adjustment value and PV the process variable value.

$$u(t) = K_p\left(e(t) + \frac{1}{T_i}\int_0^t e(t)\,dt + T_d\frac{de(t)}{dt}\right) \tag{9}$$

$$e(t) = SP - PV \tag{10}$$

To solve integral and derivative portions of Eq. 9, it was necessary to use some numerical methods. The integral part was solved using a trapezoidal approximation and the derivative part was solved using an equation of finite differences. With these techniques implemented, the final equation of control was like Eq 11 (National, 2001).

$$u(t) = K_p\left\{e(k) + \frac{1}{T_i}\sum_{i=1}^{k}\left[\frac{e(i)-e(i-1)}{2}\right]\Delta t + \frac{T_d}{\Delta t}\left[e(k)-e(k-1)\right]\right\} \tag{11}$$

Since the adjustment value of the set point can change instantaneously, the error is also subject to abruptly change in the shape of the step. These sudden changes in the error introduce an infinite value in the derivative part of the equation, impossible to be achieved. An alternative to avoid this kind of "spike" in the control signal was to use the derivative part of the equation upon the changes in process variable, instead of the error. This caused the derivative part to be according to Eq. 12 and the control equation to be changed to Eq. 13.

$$u_d(t) = K_p\left(Td\frac{d(SP(t)-PV(t))}{dt}\right) = K_p\left(-Td\frac{d(PV(t))}{dt}\right) \tag{12}$$

$$u(t) = K_p\left\{e(k) + \frac{1}{T_i}\sum_{i=1}^{k}\left[\frac{e(i)-e(i-1)}{2}\right]\Delta t - \frac{T_d}{\Delta t}\left[PV(k)-PV(k-1)\right]\right\} \tag{13}$$

Another additional aspect considered in the controller implementation was the actuator saturation, and it would be prudent to restrict the output signal to the operating range of the thermal module. A second aspect is related to the integrative part of the controller. As the integrative part counts the process errors to define the control action, the final value of the integrative parcel may be too high and may command the control action upon the integrative and derivative parts. This phenomenon is known as "Wind Up" and can be circumvented with software restrictions such as "conditionally freeze integrator", cited by Visioli (2003), which does not allow the increasing of the absolute value of

the integrative part, in the event of actuator saturation or otherwise, with the "integrator limiting" that defines an operating range for the integrative parcel. In this study, both methodologies were used.

5. RESULTS

To evaluate the variable gain control system two tests were performed. The first one with the proposed variable gain controller and the second one with fixed gain controller, where the Set Point was set from 18 º C to 16 ° C and then from 16 º C to 14 º C, as can be seen in Fig.10. The curve “Int Temp-F Gain” is the system response to step using the fixed gain controller and “Int Temp-V Gain” curve is the system response using the variable gains.

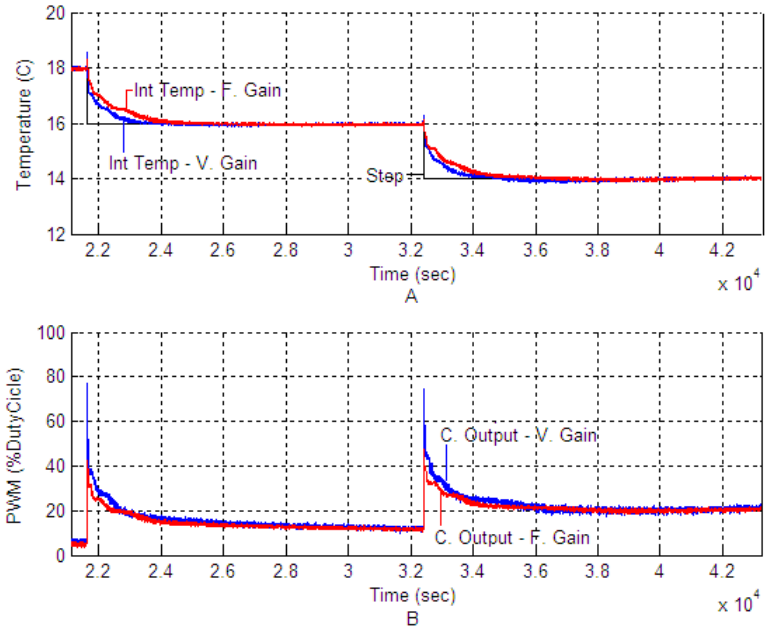

Figure 10 Fixed x Variable Gain Response

In Fig. 11 is shown with higher definition the curve in the stabilization region. Observe that the variable gain controller reached 63% of adjusted value about 5.5 minutes faster than the fixed gain controller; also, the adaptive gain adjustment has shown an average response time approximately 20 minutes faster when compared to the fixed gain controller. In both tests, the overshoot is virtually imperceptible, less than 0.2C, however it is possible to observe in Fig. 11 that the adaptive adjustment oscillates closer to the set point of 16 ºC than the variable gain controller.

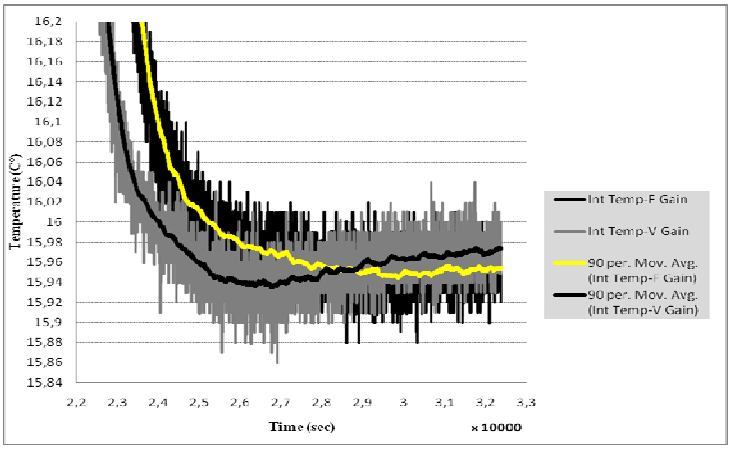

Figure 11 Fixed x Variable Gain Response with Trend line

It’s important to report that in the response curves it was observed that at the exact moment of the step application, the abrupt change of electric current applied to the module caused an electrical noise on the temperature sensors, which resulted in a deviation in the temperature measurement. Therefore, to avoid this problem in future works, the BC337

(Q6) transistor of Fig.4 will be replaced by a photo-transistor as those used for switching the H bridge mosfets, (U1) (U2) (U3) and (U4) in the same Fig.4. The aim of such change is electrical isolation between the processing and data acquisition sections from the drive section of the thermoelectric module, in which the intensity of the currents are much higher than those of the other circuit sections. Higher electric currents imply in higher electro-magnetic noises. In Fig.12, the noise region is highlighted. It is noted that the noise intensity is better observed in the step moment, were the power applied to the actuator has more significant changes.

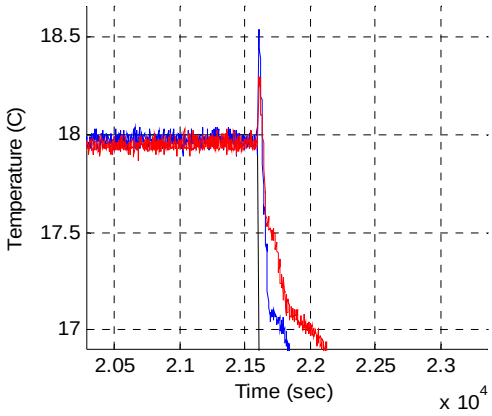

Figure 12. Noise Disturbance

6. CONCLUSION

Actually it was expected that a variable gain controller had better performance than the fixed gain controller, since the variable gain controller operates the system in accordance with the operating point and being able to determine the best parameters for the present condition of system.

In general, it is concluded that the methodology applied in this project worked well, being able to develop a variable gain controller with better performance than the fixed gain one. The comparison between tests report a response time, about 40% faster, and a smaller final error, about 0.02C, for the adaptive gain controller.

7. REFERENCES

Lio, T., Yao, K. and Gao, F., 2009, “Identification and Autotuning of Temperature-Control System With Aplication to Ingection Molding”, Proceedings of the IEEE Xplore Transaction on Control Systems Technology, Vol.17, pp. 1282-1294.

Maia, Antônio A. T., 2010, “Control of na Eletronic Expansion Valve Using an Adaptive PID Controller”. International Refrigeraion and Air Conditioning Conference at Purdue, p2387.

National, 2001, “PID control tool set user manual”, National Instruments Corporation, USA, 180p.

National, 2008, “Precision Temperature Sensors”, National Instruments Corporation, USA, 1p.

Ogata, K., 2003, “Engenharia de controle moderno”, Prentice Hall, São Paulo, Brazil, 4ª ed., 788p.

Vilanova, R., 2008, “IMC based Robust PID design: Tuning guidelines and automatic tuning”. Journal of process control, Vol. 18, pp. 61-70.

Visioli, A., 2003, “Modified Ant-WindUp Scheme for PID Controller”, Proceedings of the IEE Xplore Control Theory and Aplications, Vol.150, pp.49-54.

8. RESPONSIBILITY NOTICE

The authors are the only responsible for the printed material included in this paper